ELSEVIER

Journal of Nuclear Materials 289 (2001) 219–226

journal of nuclear materials

www.elsevier.nl/locate/jnucmat

Preliminary study of irradiation effects on thorium phosphate-diphosphate

E. Pichot [a], N. Dacheux [a,*], J. Emery [b], J. Chaumont [c], V. Brandel [a], M. Genet [a]

[a] *Groupe de Radiochimie, Institut de Physique Nucléaire, Bât. 100, Université de Paris-Sud, F-91406 Orsay cedex, France*
[b] *Laboratoire de Physique de L'Etat Condensé (UPRESA 6087), Université du Maine, av. Olivier Messiaen, F-72017 Le Mans, France*
[c] *CSNSM IN2P3 – CNRS, Bât. 104 – 108, Université de Paris-Sud, F-91406 Orsay cedex, France*

Received 12 December 2000; accepted 17 January 2001

Abstract

Thorium phosphate-diphosphate (TPD): $Th_4(PO_4)_4P_2O_7$ is proposed as a host matrix for the long-term storage of high level radioactive wastes. Indeed, γ-rays, α and β particles due to the incorporated actinides or fission products will certainly produce several effects, particularly structural and chemical modifications, in the host material. In order to investigate these effects, powdered samples were irradiated with 1.5 Gy dose of γ-rays. The formation of PO_3^{2-} and $POO^{\cdot}$ free radicals was detected using electron spin resonance (ESR) and thermoluminescence (TL) methods. These free radicals do not modify the macroscopic properties of the TPD and disappear when the sample is heated at 400°C. The implantation of He^+ ions of 1.6 MeV (fluence: 10^{16} particles cm^{-2}) and Au^{3+} ions of 5 MeV (fluence 4×10^{15} particles cm^{-2}) causes some damages on the surface of sintered samples. Amorphization and chemical decomposition of the matrix were observed for the dose of 10^{15} particles cm^{-2} and higher when irradiated with Pb^{2+} (200 keV) and Au^{3+} (5 MeV) ion beams. These effects were evidenced by means of X-ray diffraction (XRD) and X-ray photoelectron spectroscopy (XPS). © 2001 Elsevier Science B.V. All rights reserved.

1. Introduction

Thorium phosphate-diphosphate (TPD), $Th_4(PO_4)_4P_2O_7$, which crystallizes with an orthorhombic cell unit (P*cam*, $Z = 2$) [1], has been proposed as an actinide-bearing phase for nuclear waste storage. Indeed, this material is very resistant to aqueous corrosion, exhibits a high thermal stability [2] and can be also loaded in situ by large amounts of tetravalent actinides [2–4].

It is well known that the α-decay could greatly affect the crystal structure in a phase containing actinides. Nevertheless, naturally occurring monazite, containing less than 1 wt% of uranium and between 2 and 14 wt% of thorium and other species, is invariably crystallized despite the high α-decay event dose they received [5–9]. Considering that the TPD could be a potential matrix for the immobilization of actinides, its behavior during irradiation steps was studied. Indeed, one of the most important properties required for this kind of matrices studied for a long-term storage is to be resistant to radiation damages. Radiation damages can affect the release of the radionuclides from waste matrix during leaching tests by increasing the surface area (e.g., microfracturing) and mainly by decreasing the thermodynamic stability of the phases induced by radiation [10]. The most prominent effect in crystalline waste phases is the radiation-induced transformation from a crystalline to an amorphous state, as a result of self-radiation damage due to the α-decay of the incorporated actinides [11]. Such an understanding is essential in the use of the TPD as an actinide host phase in ceramic nuclear waste forms.

The radiation interactions fall into two main categories: the transfer of energy to electrons (ionization and electronic excitations) and the transfer of energy to atoms, primarily by ballistic processes involving elastic

* Corresponding author. Tel.: +33-1 69 15 73 42; fax: +33-1 69 15 71 50.
E-mail address: dacheux@ipno.in2p3.fr (N. Dacheux).

0022-3115/01/$ - see front matter © 2001 Elsevier Science B.V. All rights reserved.
PII: S0022-3115(01)00437-8

collisions and causing direct atomic displacements. Partitioning of the energy between electronic and nuclear losses is an important process controlling the radiation effects. In an α-decay event a high energy particle (~4–6 MeV), with a range of about 10 μm, and an energetic nucleus recoil (~0.1 MeV) with a range of about 20 nm, interact with the neighbor atoms and modify the periodicity of the crystalline matrix. Nearly, all the energy of the nucleus recoil is lost through elastic collisions with atoms in the structure and produces highly localized damage (a displacement cascade) with about a thousand atomic displacements. On the other hand, the α-particle dissipates most of its energy by ionization processes, but still undergoes enough elastic collisions near the end of its path to produce a few hundreds of isolated atomic displacements [12]. For β-particles and γ-rays the energy transfer is dominated by the ionization process.

Weber et al. [13] have completed a detailed study of the radiation-induced crystalline–amorphous transition in zircon in which they made a comparison between damage caused by the actinides incorporated in situ and ion-beam irradiation. They showed that amorphization dose deduced from the ion-beam irradiation and from the α-decay for ^{238}Pu-doped zircon are nearly identical. The results obtained suggest that the amorphization process in zircon is largely independent of the radiation source and of the dose rate.

This paper summarizes the results of the preliminary investigations of γ-ray and ion-beam irradiations of the TPD. On one hand, sintered pellets of pure TPD were irradiated with 1.6 MeV He^+ particles and with 200 keV Pb^{2+} ions in order to simulate the actinide α-decay. On the other hand, samples were irradiated with 5 MeV Au^{3+} ions (path range ≈ 1 μm) with a fluence between 10^{14} and 4×10^{15} particles cm^{-2} to evaluate the effect of this parameter on the structure. These experiments were completed by γ-ray irradiation studies on powdered TPD samples. Samples were irradiated with a ^{137}Cs source with a dose of 1.5×10^6 Gray. Then, the samples were analyzed by electron spin resonance (ESR) and thermal luminescence (TL) techniques.

These results were compared with those obtained by self-irradiation damage from the α-decay of ^{239}Pu in the $Th_3Pu(PO_4)_4P_2O_7$ solid solutions [3].

2. Experimental procedure

2.1. Synthesis

TPD: $Th_4(PO_4)_4P_2O_7$ can be synthesized through different ways [1,14]. One of them involves the precipitation of a precursor, the thorium phosphate-hydrogen phosphate (TPHP): $Th_2(PO_4)_2HPO_4 \cdot nH_2O$ ($n = 3$–7). It was prepared starting from a mixture of 0.5–2 M solutions of concentrated thorium nitrate (or chloride) and $(NH_4)_2HPO_4$ at pH = 9–9.5 considering a mole ratio of $\mathbf{r} = PO_4/Th = 3/2$. The precursor could be loaded with radionuclides using the co-precipitation process for high concentrations or an ion exchange process for low concentrations [15,16]. After heating in air between 800°C and 1200°C, the TPHP is transformed into $Th_4(PO_4)_4P_2O_7$ in which the radionuclides are definitively immobilized.

All the TPD samples were obtained by calcination of the TPHP in air in a PYROX MDB15 furnace. Powdered or sintered samples were heated in alumina crucibles with a heating rate equal to 5°C min^{-1}.

The sintered pellets of TPD were prepared by using an uniaxial pressing at room temperature on the powdered TPHP at 300 MPa then heating at 400°C for 5 h and up to 1100°C for 10 h. The final density of the TPD pellets obtained varies from 90% to 97% of the value calculated from the X-ray diffraction (XRD) data ($d_{calc} = 5.19$).

2.2. Apparatus and methods of characterization

Powdered samples were irradiated, at room temperature, with γ-rays using a ^{137}Cs source with a dose of 1.5 MGy (determined by Fricke dosimeter) during 48 h.

All TL studies were performed at constant heating rate equal to 10°C s^{-1}. An optical filter centered at 325 nm with a line width of 50 nm was used.

The ESR spectra were recorded with a Brucker spectrometer operating at X-band (9.5 GHz). The first derivative of the electron paramagnetic resonance absorption versus the magnetic field was thus obtained. Typical values for the microwave power were around 0.5 mW and 1 G for the amplitude modulation. For the studies performed at 100 K, a liquid-nitrogen Dewar was used. For other studies, the temperature was controlled using a nitrogen gas-flow variable temperature controller.

The simulations of the spectrum were carried out making the assumption that statistical distributions in hyperfine coupling constants exist in the TPD [17]. The free parameters used in the simulations include the main components of the **g** matrix ($g_{//}, g_{\perp}$) and the main components of the hyperfine matrix ($A_{//}, A_{\perp}$). The magnetic resonance field is calculated using the perturbation theory up to the second order.

Sintered samples were irradiated by 200 keV Pb^{2+}, 1.6 MeV He^+ and 1, 3, 5, 7 and 9 MeV Au^{n+} (with $n = 1$, 2, 3, 4 and 5, respectively) ion beams using IRMA or ARAMIS accelerators [18]. Ion-beam currents were maintained at about 0.2 μA cm^{-2}.

The XRD diagrams were collected with a Philips PW 1050/70 diffractometer using the Cu K_α ray ($\lambda =$ 1.5418 Å).

A Leybold LHS10 spectrometer was used for the X-ray photoelectron spectroscopy (XPS). All the X-ray photoelectron spectra were produced using the unmonochromated Mg K_α radiation (1253.6 eV). The spectrometer energy scale was internally calibrated using Cu ($2p_{3/2}$) (932.7 eV) and Au ($4f_{7/2}$) (84.0 eV) core level peaks. Binding energies have been referenced to C (1s) binding energy from adventitious carbon (284.8 eV). Photoelectron spectra were recorded from Th (4f), P (2p), O (1s) and C (1s) levels. High-resolution XPS scans were curve-fitted and the peak area intensities of the core levels were normalized to their respective atomic sensivity factors [19]. For a given element, a relative amount compared to its normal abundance in the pure TPD was defined. In this way, the obtained values are equal to 1 for all elements. Nevertheless, because of the atmospheric pollution we observed that the oxygen value was equal to about 1.03 ± 0.01 whereas thorium and phosphorous reached 0.94 ± 0.01.

Modifications of the surface profile of the samples irradiated with Au^{n+} ions were measured with a Dektak apparatus. The results were compared with the surface profile obtained before irradiation with an average roughness of ± 200 Å.

The scanning electron microscopy (SEM) was performed using a JEOL JMS 840 apparatus.

The partitioning of the energy loss by particles between electron and nuclear interactions and the distribution of displaced atoms were determined by computational approaches with the TRIM-96 program [20]. The $(dE/dX)_{elect}$ and $(dE/dX)_{nucl}$ values and the average number of atomic displacements as well as the particle range in the TPD were estimated from full cascade Monte Carlo calculations for all ion-beam irradiations assuming a threshold displacement energy of 25 eV [21] and a density of 5 g cm^{-3}.

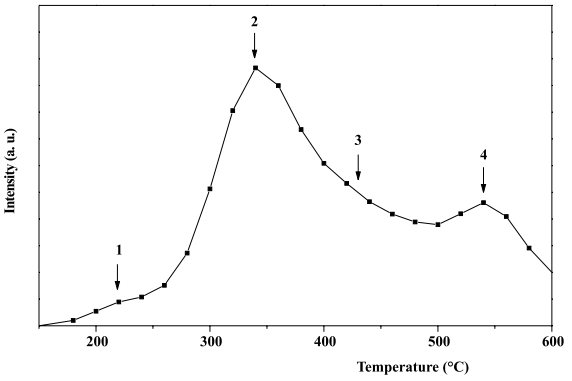

Fig. 1. TL glow curve of the TPD γ-irradiated sample. Peaks are indicated by arrows and numbers.

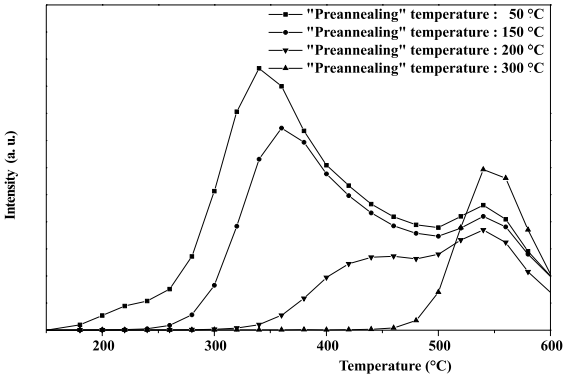

Fig. 2. TL glow curve of TPD γ-irradiated samples versus annealing temperature (experimental results obtained for 'preannealing' temperature equal to 400°C are not shown and correspond to the *X* axis).

3. Results and discussion

3.1. Results of γ-irradiation

Despite the considerable difference in the relative sensitivity of TL and ESR measurements, a strong correlation between the two types of studies was observed. Using both techniques, the irradiated samples were treated during 5 h at several temperatures before their analysis in order to point out the existence of annealing steps. This way of doing will be called further 'preannealing' [22].

The TL glow curve of the TPD samples irradiated with γ-rays at room temperature (dose = 1.5 MGy) showed the presence of four glow peaks (Fig. 1). After the preannealing step, we observed that each peak is independent (Fig. 2) and disappears at annealing temperature as reported in Table 1. The irreversible vanishing of the spectrum is due to thermal bleaching where electrons or holes are removed from their traps to recover their initial energetic states.

Furthermore, several checks performed on the TPD seem to indicate that almost identical TL spectra are obtained for γ-ray irradiated samples as for an unirradiated compound. Thus, the TL technique is sensitive enough to detect the defect amount produced in TPD by natural thorium radioactivity after 2 months ($\approx 10^{10}$ α-decay g^{-1}) of self-irradiation. This also suggests that the damages produced by the α-decay of thorium lead to defects of the same nature as those generated by γ-ray. In the same conditions, the ESR spectrum of the raw sample did not show the presence of any paramagnetic species prior to irradiation.

The modification of the ESR spectra versus the preannealing temperature for TPD γ-irradiated samples is reported in Fig. 3. The spectrum obtained at room temperature presents three distinct components (3135,

Table 1
Annealing temperature for the glow peaks

Peak number	Heating temperature (°C)
1	100
2	200
3	250
4	400

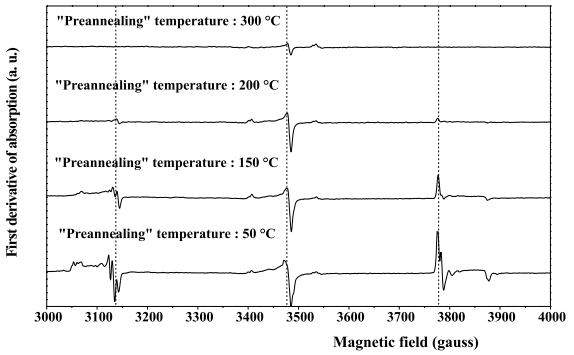

Fig. 3. Modification of ESR spectra versus annealing temperature for TPD γ-irradiated samples.

3480 and 3780 G) including a pair of hyperfine lines due to the ^{31}P interaction. The pair of hyperfine lines due to the ^{31}P interaction (doublet) of the spectrum obtained at room temperature is presented in Fig. 4. After heating at 150°C, we observed the modification of the doublet and beyond 300°C, only the central component (3480 G) is still present. No defects, leading to an ESR signal, were observed for temperatures higher than 400°C. The thermal study showed the presence of three independent doublets (pointed by arrows: 1–1, 2–2, 3–3) corresponding to three different paramagnetic sites in the

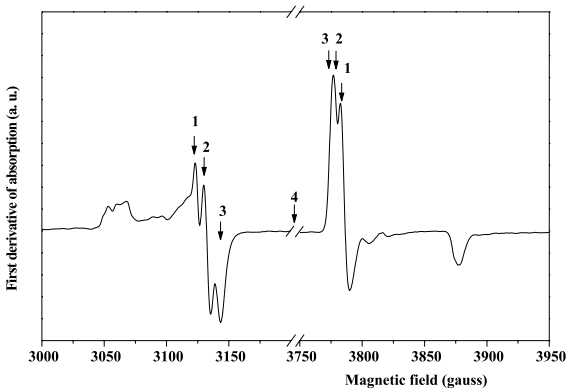

Fig. 4. X-band ESR spectrum of the PO_3^{2-} defect in TPD following γ-irradiation. Spectral components are indicated by the same notations as reported in Table 1 according to the TL results.

powdered sample. We also determined the range of annealing temperatures for each defect. Because values of the annealing temperature obtained by ESR are in relation with the information given from the TL study, we proposed to correlate these defects with those observed by TL (Table 1).

As previously described, for irradiated phosphates [23], this type of doublet defect may have a structure comparable to the PO_3^{2-} molecular ion and this defect is suggested as the phosphorus analog of the silicon (Si) E' center [24]. The model of the E' center which is generally accepted is a hole trapped at the site of an oxygen vacancy. Specifically, Feigl et al. [25] argued that the precursor of the E' center must be an oxygen vacancy containing two electrons. When one of the electrons is removed (a hole is created and trapped) the resulting paramagnetic center is stabilized by an asymmetric relaxation between two silicons or equivalent two phosphorus atoms [26].

Considering the central spectral component, it is clear that the remaining oxygen bond cannot be shared with the phosphorus atom, because this should result in a hyperfine interaction between the nuclear and electron spin of the phosphorus atom which is not observed in the spectrum. Conclusively, it seems that the responsible center for the central signal is the peroxo radicals, corresponding to trapped holes on oxygen atoms at the end of a short chain P–O–O· [27]. The presence of peroxo radicals is a strong evidence for the pre-existence of precursor structures in the TPD which are assumed to be peroxo linkages P–O–O–P and/or P–O–O–Th [27,28]. From this assumption concerning the nature of the defects, it is possible to simulate the ESR spectrum.

The free parameters obtained by simulation of the ESR spectrum are reported in Table 2. Fig. 5 represents the fit of one part of the doublet. Assuming the presence of three independent PO_3^{2-} defects, the results seem to be in rather good accordance with the experimental spectrum. The relatively bad agreement at low field component (3040–3080 G) could be due to some disorder or some anisotropy of the g tensors between the three different sites.

For the low temperature irradiation and measurements (about 100 K) a signal assigned to the phosphorus

Table 2
Values of ESR parameters obtained by computer simulations to fit with the observed TPD γ-irradiated spectrum

	Doublet			Singlet
Defect nature	PO_3^{2-}	PO_3^{2-}	PO_3^{2-}	POO·
ESR notation	3	2	1	4
$g_{//}$	1.998	1.998	1.997	2.005
$g_{\perp}$	1.998	1.998	1.997	2.010
$A_{//}$ (G)	810	815	815	0
$A_{\perp}$ (G)	635	646	658	0

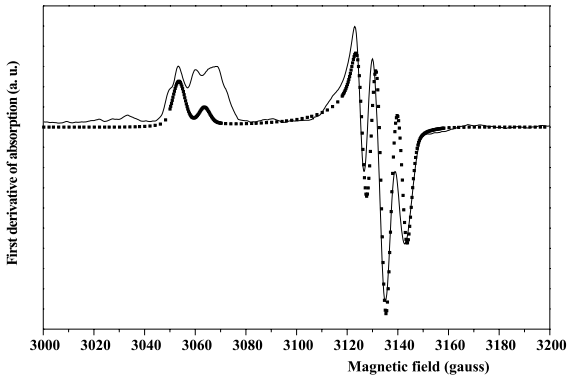

Fig. 5. X-band ESR spectrum of a part of the PO_3^{2-} defect in TPD following γ-irradiation. Dotted curve is a computer line shape simulation as explained in the text.

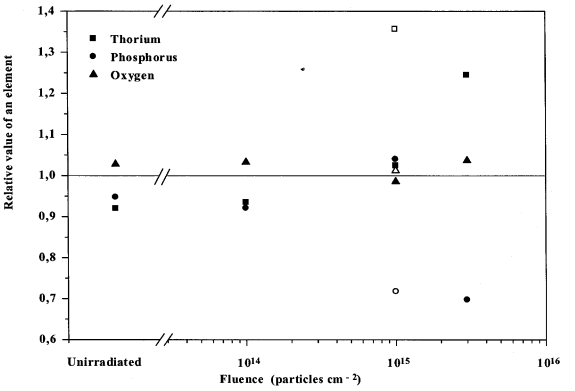

Fig. 6. Relative amount of thorium (■), phosphorus (●) and oxygen (▲) compared to pure TPD versus fluence (particles cm^{-2}) for 200 keV Pb^{2+} irradiation. Empty symbols represent results from 5 MeV Au^{3+} irradiation.

oxygen hole center ('POHC'), or PO_4^{2-} radical, is observed for a dose of 500 Gy γ-irradiation [29]. The spectrum is broadened beyond the limits of detection. It disappeared by warming the sample above 25°C and reappeared by cooling below this temperature. Subramanian et al. [30] observed a similar result for γ-irradiated phosphate-doped calcium tungstate. No defects, leading to an ESR signal, exist for temperatures over 100°C.

Finally, for 1.5 MGy γ-irradiation, it was verified by the XRD method that TPD was still well crystallized. Nevertheless, this type of macroscopic tests is not enough to definitely prove that the TPD is still unchanged.

3.2. Results of ion-beam irradiation

Sintered pellets of pure TPD were irradiated with 1.6 MeV He^+ particles and 200 keV Pb^{2+} ions in order to simulate the actinide α-decay effects. The XPS was used to determine the stoichiometry of the TPD irradiated surface as a function of the particle fluence. We did not observe any effect of He^+ irradiations for the fluence values between 10^{14} and 10^{16} particles cm^{-2}. The TPD is still crystallized and XPS studies showed no significant modification of the surface stoichiometry. For Pb^{2+} ions irradiation, the thorium and phosphorus surface stoichiometries are clearly modified for fluences higher than 10^{15} particles cm^{-2}. The surface appears as thorium enriched by comparison to the raw sample (Fig. 6). These results could be interpreted as pure ballistic sputtering involving elastic collisions. However, another type of interaction, involving electron energy loss processes [31], also has been demonstrated to be important in the ion-beam irradiation of insulating phosphate ceramics.

In order to observe the electron energy density loss effect, we chose to irradiate samples by 5 MeV Au^{3+} at different fluences. The irradiation of the sample with Au^{3+} ions at fluences between 3×10^{13} and 4×10^{15} particles cm^{-2} led to the formation of visible surface modification as evidenced by the SEM micrograph (Fig. 7). Furthermore, it was established, by means of surface profile measurements, that Au^{3+} irradiation of the TPD led to the formation of a hole. Fig. 8 shows the 'hole depth' as a function of the fluence, with a precision of about ±200 Å as observed on an unchanged surface. No measurable modification of the surface profile was observed for fluences lower than 3×10^{13} particles cm^{-2}. For higher fluence values, a linear increase of the hole depth is observed followed by saturation effect at doses around 10^{15} particles cm^{-2} which may be related to an equilibrium state. XPS has been used to determine the chemical surface stoichiometry of the TPD irradiated with 5 MeV Au^{3+} ions at a fluence of 10^{15} particles cm^{-2}. The results are given in Fig. 6. The surface appears as thorium enriched as it was previously observed using Pb^{2+}-ion irradiations.

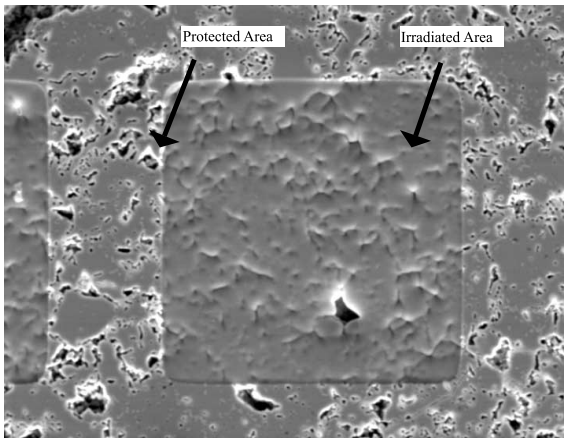

Fig. 7. SEM micrograph of TPD irradiated pellets by 5 MeV Au^{3+} ions at the fluence of 4×10^{15} (particles cm^{-2}).

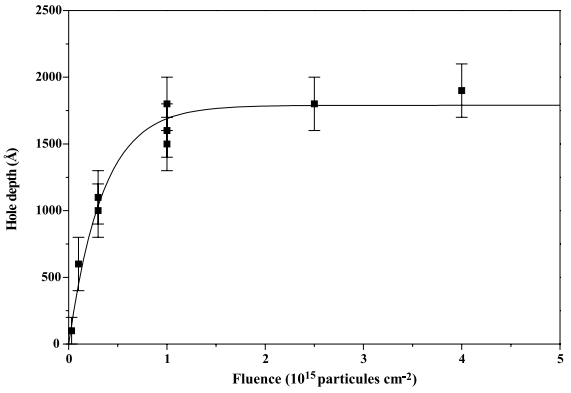

Fig. 8. 'Hole depth' as a function of the fluence for 5 MeV Au^{3+} ion irradiation (precision about ±200 Å).

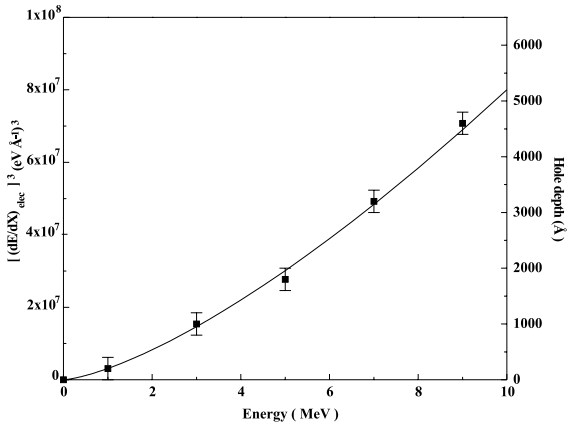

Fig. 9. 'Hole depth' as a function of the energy of Au^{n+} ion irradiation at the fluence of 10^{15} (particles cm^{-2}). Results are compared with the $(dE/dX)_{elect}$ cubic function.

Considering both studies, electronic energy loss seems to be the main process in the modification of the surface chemical stoichiometry of TPD samples. This is in accordance with the calculated characteristics of the Au^{n+} ions in terms of energy (Table 3).

The variation of the hole depth as a function of the Au^{n+} ion irradiation energy at a constant fluence of 10^{15} particles cm^{-2} (saturation value) is reported in Table 4 and in Fig. 9. The 'compaction' percentage was calculated as the ratio of the hole depth over the ion range. Taking into account the large effect observed, a mechanism based on sputtering was suggested. The number of sputtered atoms per particles (calculated from the hole depth values and the TPD atomic density) increases as the third power of $(dE/dX)_{elect}$ (Fig. 9 solid line). Studies on leucine molecules showed the same power dependence of this parameter [32] and a similar behavior has been observed for Eu_2O_3 [33] with particle energy of about 1 MeV amu^{-1}. In our study particle energy are lower than 0.05 MeV amu^{-1}.

Some authors proposed several models in order to explain how the deposition energy in the electron system is converted into atomic or molecular motion and how this excitation of the atomic system leads to the desorption at the surface [34–36]. In the thermal spike model, the energy of secondary electrons produced by ionization is transferred to the lattice via electron–phonon coupling [37,38]. A local rise of temperature appears which is proportional to the electron stopping power of the incident ions. Applied to the TPD, the ion projectile is probably transformed, after the impact, into a hot neutral plasma leading to the evaporation of the phosphoric oxide. This process could be compared to the already described thermal decomposition of the TPD [1]

Table 3
Characteristics of Au^{n+} irradiations as a function of the energy determined by the TRIM code

Energy (MeV)	Ion charge	$(dE/dX)_{elec}$ (eV Å^{-1})	$(dE/dX)_{nucl}$ (eV Å^{-1})	Path range (μm)
1	1	155	390	0.18
3	2	260	300	0.49
5	3	330	240	0.80
7	4	390	200	1.12
9	5	440	180	1.42

Table 4
Hole depth as a function of the Au^{n+} particle energy and associated calculated 'compaction' and number of atoms sputtered per impact

Energy (MeV)	Hole depth (Å)	Compaction (%)	Number of atoms sputtered (per impact)
1	200	11	130
3	1000	23	660
5	1800	23	1200
7	3200	29	2100
9	4600	30	3000

$$Th_4(PO_4)_4P_2O_7 \rightarrow ThO_2 + (ThO)_3(PO_4)_2 + P_4O_{10} \uparrow . \quad (1)$$

The chemical decomposition of irradiated materials is usually observed. For example, the formation of calcium oxide (CaO) was found when single crystals of natural fluoroapatite were irradiated by an electron beam in a transmission electron microscope using high current density (16 A cm^{-2}) [39–41]. Meldrum et al. [39] observed many beam-induced bubbles enriched in phosphorus in comparison with the crystalline apatite. This observation is in good agreement with our XPS results which concluded the depletion of phosphorus.

The TPD is proposed as matrix for actinide immobilization thus, it is necessary to check which process occurs in the matrix, loaded with a large amount of actinides. In this objective, a solid solution of thorium–plutonium (IV) phosphate-diphosphate (TPuPD) containing 16 wt% of ^{239}Pu ($Th_3Pu(PO_4)_4P_2O_7$) was synthesized and stored during 3 years. The XRD diagram of the sample was recorded on the compound freshly prepared and, then, after 16 and 36 months of storage. No differences were observed between these diagrams. The calculated number of α-decay events corresponds to about 3×10^{16} disintegrations per gram of TPuPD solid solution after 3 years. The cumulative dose could be expressed in units of displacements per atom (dpa) [42] to allow the comparison of the damage produced from irradiations of different natures and energies. Expressing the cumulative dose in dpa the value is equal to about 0.008 dpa. Under 5 MeV Au^{3+} ion-beam irradiations, TPD undergoes the crystalline-to-amorphous transition at room temperature, with the completely amorphous state obtained for an ion fluence of 10^{14} particles cm^{-2}, which correspond to about 0.4 dpa (Fig. 10). Thus, in order to reach this dpa level in the TPuPD solid solution, the use of ^{238}Pu (α, $T_{1/2} = 87.7$ years) instead of ^{239}Pu (α, $T_{1/2} = 24\,500$ years) is required. This study could also emphasize the rôle played by the dose rate, because in many compounds α-decay damages may be partially recovered by the point defect migration over periods of time [40,43].

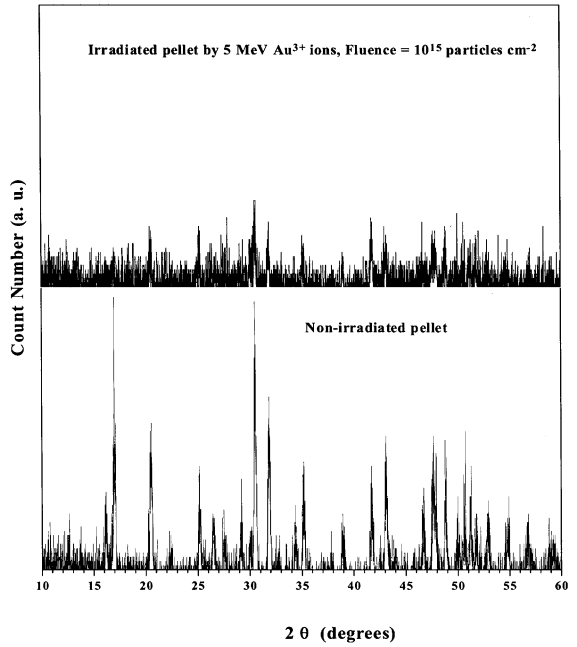

Fig. 10. X-ray diffraction diagram comparison between non-irradiated and 5 MeV Au^{3+} ion-irradiated pellets at the fluence of 10^{15} (particles cm^{-2}).

A re-crystallization process, between 500°C and 1000°C, of the completely ion-beam amorphisized TPD samples, was observed by means of XRD. The identification of the compound was performed on a re-crystallized sample by comparison with the JCPDS – International Center for Diffraction Database and the DIFFRACT-AT search program supplied by Siemens. No other phase was observed in the annealed solid.

4. Conclusions

In the framework of the long-term repository of radioactive wastes, including actinides, new matrices with a very high resistance to aqueous corrosion are needed. Considering this first stringency, TPD is probably one of the best matrices studied at present time. The second criterion is the behavior of the actinide-bearing phase under irradiation. For this, irradiation effects on TPD were studied using 200 keV Pb^{2+} and 1.6 MeV He^+ particle beams in order to reproduce α-decay effects and by more energetic irradiation in order to have a better understanding of these effects associated to the electron energy loss processes. The results were obtained from different methods depending on irradiation sources and effects (XPS, XRD, SEM, etc.).

XPS allowed to observe that heavy particles with an energy of around 100 keV modified the chemical stoichiometry at the surface of the sintered samples. It might be interpreted as a pure ballistic differential sputtering effect involving elastic collisions. The same results were observed in the case of Au^{n+} irradiation at higher energy (between 3 and 10 MeV) but the effect looks to be related to the electronic stopping power. At the same time, the formation of holes at the surface of the samples was observed for fluence values lower than 10^{15} particles cm^{-2}. Only the interaction involving electron energy loss processes could explain the high evaporation process observed and the modification of the chemical surface stoichiometry.

Furthermore, the γ-irradiation (1.5 MGy) of powdered sample induced the presence of paramagnetic defects. Following a preannealing step, we observed by

ESR and thermoluminescence (TL) method the decrease of the corresponding signals. By correlation between these two techniques, we identified four independent types of defects and determined their annealing temperatures (Table 1, Fig. 1).

In this preliminary study of irradiation effects on the TPD, we have observed the main effects of an α-decay, using the ion-beam accelerator technique. Nevertheless, the study of damage recovery is necessary in order to be able to extrapolate these results to the time required for a long-term repository. Thus, the X-ray pattern of a solid solution (TPuPD) doped with 16 wt% of ^{239}Pu and stored during 3 years was recorded. Neither modification of the peak position nor of the FWHM values was observed. The corresponding irradiation dose given in dpa was calculated to be equal to 0.008 dpa which is 2 orders of magnitude lower than the amorphization dose determined from ion-beam irradiation. Another study with a solid solution synthesized with 10 wt% of ^{238}Pu is necessary to increase this dpa level.

Acknowledgements

One of us would like to thank Dr J.C. Dolo, CEA–Saclay, for his help in ESR experiments and Dr C. Severac, University of Paris-Sud–Orsay, for the XPS studies.

References

[1] P. Benard, V. Brandel, N. Dacheux, S. Jaulmes, S. Launay, C. Lindecker, M. Genet, D. Louer, M. Quarton, Chem. Mater. 8 (1996) 181.
[2] N. Dacheux, A.C. Thomas, B. Chassigneux, E. Pichot, V. Brandel, M. Genet, Mater. Res. Soc. Symp. Proc. 556 (1999) 85.
[3] N. Dacheux, R. Podor, V. Brandel, M. Genet, J. Nucl. Mater. 252 (1998) 179.
[4] N. Dacheux, A.C. Thomas, V. Brandel, M. Genet, J. Nucl. Mater. 257 (1998) 108.
[5] R.C. Ewing, Am. Miner. 60 (1975) 728.
[6] R.C. Ewing, in: Metamict Mineral Alteration: an implication for radioactive waste disposal, USERDA Report no. Conf-770102.
[7] R.C. Ewing, R.F. Haaker, Nucl. Chem. Waste Management 1 (1980) 51.
[8] R.J. Floran, M.M. Abraham, L.A. Boatner, M. Rappaz, in: J.G. Moore (Ed.), Scientific Basis for Nuclear Waste Management, Vol. 3, 1981, 507.
[9] Y. Eyal, D.R. Olander, Geochim. Cosmochim. Acta 54 (1990) 1867.
[10] W.J. Weber, R.C. Ewing, C.R.A. Catlow, T. Diaz De La Rubia, L.W. Hobbs, C. Kinoshita, Hj. Matzke, A.T. Motta, M. Nastai, E.K.H. Salje, E.R. Vance, S.J. Zinkle, J. Mater. Res. 13 (1998) 1434.
[11] W.J. Weber, Hj. Matzke, Radiat. Eff. 98 (1986) 93.
[12] L.W. Hobbs, F.W. Clinard, S.J. Zinkle, R.C. Ewing, J. Nucl. Mater. 216 (1994) 291.
[13] W.J. Weber, R.C. Ewing, L. Min Wang, J. Mater. Res. 9 (1994) 688.
[14] V. Brandel, N. Dacheux, E. Pichot, M. Genet, J. Emery, J.Y. Buzare, R. Podor, Chem. Mater. 10 (1998) 345.
[15] E. Pichot, N. Dacheux, V. Brandel, M. Genet, New J. Chem. 24 (2000) 1017.
[16] V. Brandel, N. Dacheux, M. Genet, E. Pichot, A.C. Thomas, in: Future Nuclear Systems Global 99, Proceedings on CD-Rom, Jackson Hole, WY, 1999.
[17] D.L. Griscom, J. Non-Cryst. Solids 13 (1973) 251.
[18] H. Bernas, J. Chaumont, E. Cottereau, R. Meunier, A. Traverse, C. Clerc, O. Kaitosov, F. Lalu, D. Ledu, G. Moroy, M. Salome, Nucl. Instrum. and Meth. B 62 (1992) 416.
[19] J. Scofield, J. Electr. Spectr. Related Phenom. 8 (1976) 129.
[20] J.F. Ziegler, 1996, TRIM Version 96.01. IBM-Research.
[21] A. Meldrum, L.M. Wang, R.C. Ewing, Nucl. Instrum. and Meth. B 116 (1996) 220.
[22] Y. Nakai, Bull. Chem. Soc. Jpn. 37 (1964) 1089.
[23] N.J. Clayden, J. Chem. Soc. Dalt. Trans. (1987) 1877.
[24] D.L. Griscom, J. Non-Cryst. Solids 179 (1994) 22.
[25] F.J. Feigl, W.B. Fowler, K.L. Yip, Solid State Comm. 14 (1974) 225.
[26] G. Paccioni, A.M. Ferrari, G. Ierano, Faraday Discuss. 106 (1997) 155.
[27] M.E. Archidi, M. Haddad, A. Nadiri, F. Benyaich, R. Berger, Nucl. Instrum. and Meth. B 116 (1996) 145.
[28] D.L. Griscom, J. Non-Cryst. Solids 40 (1980) 211.
[29] R.A. Serway, S.A. Marshall, J. Chem. Phys. 45 (1966) 4098.
[30] S. Subramanian, M.C.R. Symons, H.W. Wardale, J. Chem. Soc. A (1970) 1239.
[31] B.C. Sales, R.A. Zuhr, J.C. McCallum, L.A. Boatner, Phys. Rev. B 46 (1992) 3215.
[32] A. Hedin, P. Hakansson, B.U.R. Sundqvist, Phys. Rev. B 35 (1987) 7377.
[33] W. Guthier, in: A. Benninghoven (Ed.), Proceedings of the Third International Workshop on Ion Formation from Organic Solids, Munster, 1985, Springer Proc. Phys. 9 (1986) 17.
[34] A. Hedin, P. Hakansson, B.U.R. Sundqvist, R.E. Johnson, Phys. Rev. B 31 (1985) 1780.
[35] I.S. Bittesky, E.S. Parilis, Nucl. Instrum. and Meth. B 21 (1987) 26.
[36] P. Williams, B.U.R. Sundqvist, Phys. Rev. Lett. 58 (1987) 1031.
[37] M. Toulemonde, E. Paumier, C. Dufour, Radiat. Eff. Def. Solids 126 (1993) 163.
[38] F. Seitz, J.S. Koehler, Solid State Phys. 2 (1956) 305.
[39] A. Meldrum, L.M. Wang, R.C. Ewing, Am. Mineral. 82 (1997) 858.
[40] R.C. Ewing, L.M. Wang, W.J. Weber, Mater. Res. Soc. Symp. Proc. 373 (1995) 347.
[41] A. Meldrum, L.A. Boatner, R.C. Ewing, Mater. Res. Soc. Symp. Proc. 439 (1997) 697.
[42] A. Meldrum, L.A. Boatner, R.C. Ewing, Phys. Rev. B 56 (1997) 13805.
[43] A. Meldum, L.A. Boatner, W.J. Weber, R.C. Ewing, Geochim. Cosmochim. Acta 62 (1998) 2509.